Observational Study

Medicine®

OPEN

Next-generation sequencing identifies a novel heterozygous I229T mutation on LMNA associated with familial cardiac conduction disease

Yuan Gao, PhD[a,b], Zhonglin Han, PhD[a], Xiang Wu, PhD[a], Rongfang Lan, PhD[a], Xinlin Zhang, MD[a], Wenzhi Shen, MD[a], Yu Liu, PhD[a], Xuehua Liu, PhD[a], Xi Lan, MM[a], Biao Xu, PhD[a], Wei Xu, MD[a,*]

Abstract

LMNA gene encodes Lamin A and C (Lamin A/C), which are intermediate filament protein implicating in DNA replication and transcription. Mutations in LMNA are validated to cause cardiac conduction disease (CCD) and cardiomyopathy.

In a Chinese family, we identified 5 members harboring the identical heterozygous LMNA (c.686T>C, I229T) disease-causing mutation, which was not found in the 535 healthy controls. In silico analysis, we revealed structural alteration in Lamin A/C I229T mutant. Furthermore, molecular docking identified human polycomb repressive complex 2 and Lamin A/C interact with higher affinity in the presence of I229T, thus may downregulate Nav1.5 channel expression.

Our findings expanded the spectrum of mutations associated with CCD and were valuable in the genetic diagnosis and clinical screening for CCD. Molecular docking analysis provided useful information of increased binding affinity between mutant Lamin A/C and polycomb repressive complex 2. However, the concrete mechanism of LMNA mutation (I229T) remains undetermined in our study, future genetics and molecular studies are still needed.

Abbreviations: AKAP9 = A-kinase anchoring protein 9, CCD = cardiac conduction disease, DCM = dilated cardiomyopathy, ECG = electrocardiography, ERK = extracellular signal-regulated kinase, ICCD = inherited cardiac conduction disease, iPSC-CMs = pluripotent stem cell-derived cardiomyocytes, LVDd = left ventricular end-diastolic diameter, LVEF = left ventricular ejection fraction, MAPK = mitogen-activated protein kinase, NGS = next-generation sequencing, PDGF = platelet-derived growth factor, PRC2 = polycomb repressive complex 2.

Keywords: cardiac conduction disease, LMNA, molecular docking, next-generation sequencing, polycomb repressive complex 2

1. Introduction

Cardiac conduction disease (CCD) is a life-threatening disorder in which the integrity of the conduction system is impaired. The pathophysiological mechanisms underlying CCD are complex, but regardless of the cause, pacemaker implantation may be the ultimate treatment. If CCD is of an inherited nature (ICCD), autosomal dominant inheritance is the predominant pattern of transmission. ICCD has extensive genetic heterogeneity and phenotypic variances including the age of onset, disease severity, and progression. Previously, several studies have demonstrated a strong correlation between ICCD and dilated cardiomyopathy (DCM).[1–3] The underlying mechanisms of its unexplained clinical variability and progression to DCM remain poorly understood.

In the recent 20 years, over 30 genes have been implicated in harboring that cause ICCD. The mutation of LMNA is one of the most common causes of ICCD and hereditary DCM. LMNA mutations are inherited in an autosomal dominant manner. It encodes Lamin A and C (Lamin A/C), which are intermediate filament proteins coupled to components of the nuclear lamina. The damage of nuclear lamina is detrimental to the nuclear membrane, and further leads to potential gene expression alteration or cardiomyocyte dysfunction. LMNA mutations were reported to be associated frequently with at least 4 different cardiac phenotypes, including conduction diseases (sinoatrial and His/bundle disease),[4] supraventricular and ventricular arrhythmias,[5] DCM,[6] and vascular thromboembolism.[7] Here, we reported a Chinese family with 5 members presented as different subtypes of CCD (Sick sinus syndrome, type-II 2nd degree AV block), 4 members with sudden death from presumed heart disease, 1 member with third-degree AV block and extensive heart enlargement. By using next-generation sequencing (NGS) and comparing the database, we confirmed that this LMNA mutation site was a new mutation site leading to ICCD.

Editor: Ovidiu Constantin Baltatu.

Funding was provided by the National Natural Science Foundation of China (No. 81600267) to Zhonglin Han.

The datasets generated during and/or analyzed during the current study are not publicly available, but are available from the corresponding author on reasonable request.

The authors report no conflicts of interest.

Supplemental Digital Content is available for this article.

[a] Nanjing Drum Tower Hospital, The Affiliated Hospital of Nanjing University Medical School, [b] Nanjing Drum Tower Hospital Clinical College of Nanjing Medical University, Nanjing, Jiangsu Province, China.

[*] Correspondence: Wei Xu, Department of Cardiology, Nanjing Drum Tower Hospital, Road Zhongshan, No. 321, Nanjing, Jiangsu Province, 210008, China (e-mail: 13390900868@163.com).

How to cite this article: Gao Y, Han Z, Wu X, Lan R, Zhang X, Shen W, Liu Y, Liu X, Lan X, Xu B, Xu W. Next-generation sequencing identifies a novel heterozygous I229T mutation on LMNA associated with familial cardiac conduction disease. Medicine 2020;99:34(e21797).

Received: 18 January 2020 / Received in final form: 21 May 2020 / Accepted: 16 July 2020

http://dx.doi.org/10.1097/MD.0000000000021797

2. Methods

2.1. Ethics statement

This study was fully in accordance with the 1964 Helsinki Declaration and the ethical guidelines of the local ethics committee at the Affiliated Drum Tower Hospital. Written informed consent was obtained from all subjects.

2.2. Study participants and clinical evaluation

A Chinese CCD family was clinically evaluated (Fig. 1). Peripheral blood samples were collected from 12 subjects: 7 individuals with non-prominent cardiac disease, 2 individuals with sick sinus syndrome, 1 individual with type-II second-degree AV block, 1 individual with complete right bundle block, 1 individual with third-degree AV block and extensive left heart enlargement. We included 535 ethnically matched healthy controls with normal electrocardiograms (ECG). Peripheral blood samples were collected for DNA analysis.

Diagnosis of CCD is based on classic signs and symptoms resting 12-leads ECG and/or ambulatory ECG monitoring, pharmacologic testing and electrophysiology testing.[8] For DCM, we evaluate the family history, physical and clinical examination, resting ECG, and echocardiography. Clinical diagnosis of DCM is according to published guidelines of evidence of systolic dysfunction and dilation of 1 or both ventricles:

(1) left ventricular end-diastolic diameter (LVDd) >5.5 cm in the male and LVDd >5.0 in the female.
(2) Left ventricular ejection fraction (LVEF) <45% (Simpson method) and/or left ventricular fractional shortening <25%.
(3) In the absence of hypertension, valvular heart disease, congenital heart disease, and ischemic heart disease.[9,10]

2.3. ECG and echocardiography

ECG and ambulatory ECG monitoring are recorded and evaluated by a senior cardiologist. Echocardiography was obtained using a Philips Sonos 5500 ultrasound system. LVEF was assessed by using the Simpson biplane method. LVDd and left atrial diameter were assessed from 2-dimensional images.

2.4. NGS

We collected the EDTA-treated peripheral blood from the consanguineous Chinese family members with informed consents. The peripheral blood genomic DNA was extracted using the DNeasy kit (Qiagen). The concentration and quality of extracted DNA samples were measured by Nanodrop 2000 spectrophotometer (Thermo scientific). Targeted NGS, including DNA library construction, capture, and sequencing, was performed by MyGenostics Gene Technologies (Beijing, China). Custom targeted gene enrichment was performed using the GenCap Custom Enrichment Kit (MyGenostics) according to the manufacturer's protocol. High-throughput sequencing was performed by Illumina NovaSeq 6000 series sequencer (PE150), and not less than 99% of target sequence was sequenced. We excluded single nucleotide polymorphisms of a

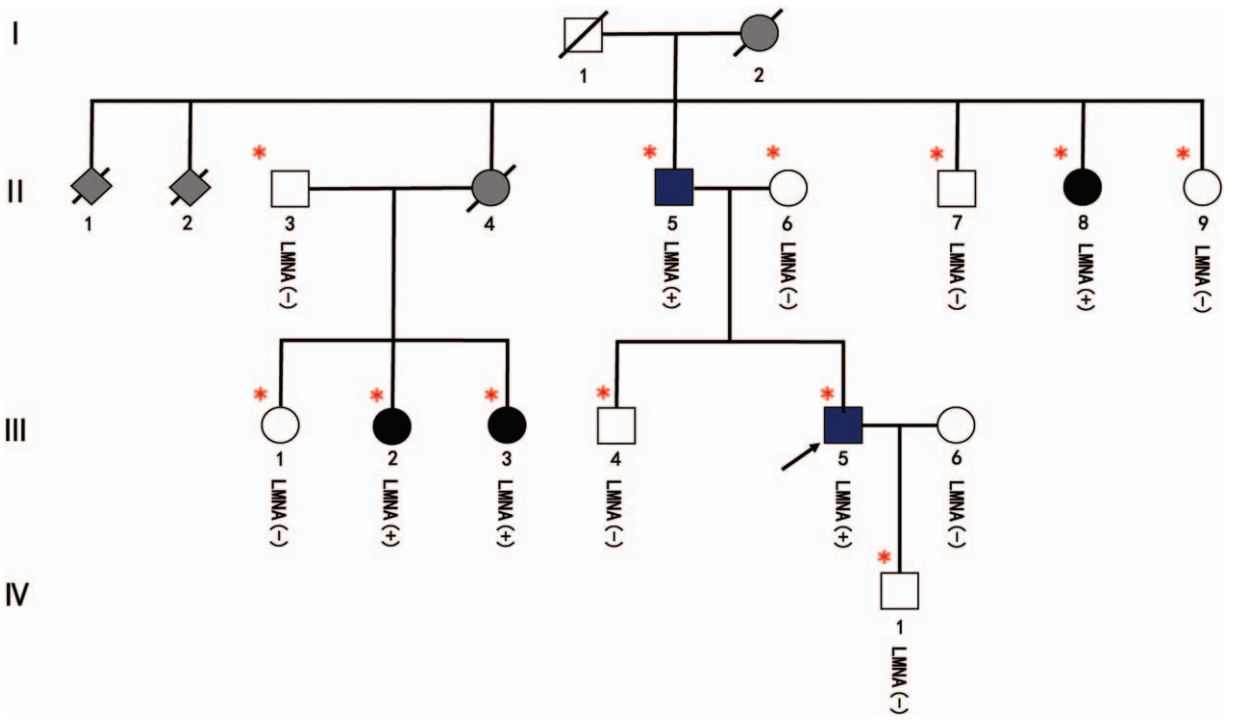

Figure 1. Pedigree of the Chinese family with inherited cardiac conduction disease. Females are depicted as circles and males as squares. Black solid squares and circles denote severely affected cardiac conduction disease members, gray solid cycle sudden cardiac death recalled as "heart disease," open squares and cycles healthy members with wild-type LMNA. Squares and circles with a crossing-slash indicate deceased individual, asterisks denote family members whose samples were sequenced and proband indicated with an arrow. Genotypes for LMNA were illustrated below the icons for each individual with a plus (+) indicating mutant and a minus (–) indicating wildtype for that genotype.

Table 1

Clinical characteristics of family members.

Patient	Sex	Age, yr	AHR, bmp	LHR, bmp	LRR, s	Cardiac Rhythm	LAD, cm	LVDd, cm	LVEF (%)
II-3	M	67	72	48	1.7	Sinus	3.6	5.3	60.0
II-5	M	72	48	24	2.7	SSS	4.5	5.3	60.0
II-6	F	68	59	43	1.5	Sinus	4.2	5.0	61.0
II-7	M	67	72	50	1.4	Sinus	3.4	4.8	62.0
II-8	F	68	47	24	4.3	SSS	4.7	5.7	55.0
II-9	F	62	83	58	1.4	Sinus	4.3	5.1	63.0
III-1	F	58	67	41	1.4	Sinus	2.8	4.6	64.0
III-2	F	55	78	60	1.0	CRBB	3.3	5.0	59.0
III-3	F	54	47	31	3.4	Type-II 2nd	2.9	4.3	65.7
III-4	M	47	77	58	1.2	Sinus	3.9	5.0	59.0
III-5*	M	42	39	21	3.9	Third-degree	4.7	6.2	53.0
IV-1	M	23	66	52	1.1	Sinus	2.9	4.4	62.0

AHR = average heart rhythm, CRBB = complete right bundle block, LAD = left atrium diameter, LHR = lowest heart rate, LRR = longest RR interval, LVDd = left ventricular end diastolic diameter, LVEF = left ventricular ejection fraction, Sinus = sinus rhythm, SSS = sick sinus syndrome, Third-degree = third-degree atrioventricular block, Type-II 2nd = type-II 2nd atrioventricular block.

quality score <20, a strand bias >60, in the exomes generated from 535 unaffected control samples and minor allele frequency (MAF) >0.2%, 0.4%, 0.05%, respectively for HCM, DCM, and ARVC (1,000 genomes, dbSNP, ESP, ExAC, and Chigene in-house MAFs database).

2.5. Bioinformatics analysis

Raw data were processed by fastp for adapters removing and low-quality reads filtering. The paired-end reads were performed using Burrows-Wheeler Aligner (BWA)[11] to the Ensemble GRCh37/hg19 reference genome. We used GATK[12] to conduct base quality score recalibration together with SNP and short indel calling. According to the sequence depth and variant quality, SNPs and Indels were screened that high quality and reliable variants were obtained. We used the online system independently developed by Chigene (www.chigene.org) to annotate database-based MAFs and ACMG practice guideline-based pathogenicity of every yielded gene variant. The system also provided a serial software package for conservative analysis and protein product structure prediction. The databases for MAFs annotation include 1,000 genomes, dbSNP, ESP, ExAC, and Chigene in-house MAFs database. We used Provean, Sift, Polypen2, MutationTaster, M-CAP, and REVEL software packages to predict protein product structure variation. As a prioritized pathogenicity annotation to ACMG guideline, OMIM, HGMD, and ClinVar databases were used as conferences of pathogenicity of every variant. We used MaxEntScan, dbscSNV, and GTAG software packages to predict the functional change of variants on the splicing sites. All potential pathogenic mutations were verified by Sanger sequencing, using primers designed from Primer Premier 5 software.

2.6. Molecular docking

Molecular docking was performed to investigate the binding mode between the human PRC2 and the human Lamin A/C (wildtype and I229T mutant) using the ZDOCK server (zdock.umassmed.edu). The 3-dimensional structures of the PRC2 (PDB ID: 5GSA) and the Lamin A/C (PDB ID: 6JLB) were downloaded from RCSB Protein Data Bank (www.rcsb.org). Human Lamin A/C I229T mutant was built using a mutagenesis module in PyMoL 1.7.6 software (www.pymol.org). For docking, the default parameters were used as described in the ZDOCK server. The top-ranked pose as judged by the docking score was subject to visually analyze using PyMoL 1.7.6.

3. Results

3.1. Description of pedigree

All CCD patients were from a Chinese family. We obtained all the available medical records from the first-degree relatives. The clinical characteristics of the family members were outlined (Table 1). The proband (III -5) came to our hospital at age 38 with repetitive lightheadedness for 2 months. Ambulatory ECG monitoring revealed permanent third-degree AV block. His transthoracic echocardiography showed normal LEVF (53%) with extensive enlargement of the left atrium (4.7 cm) and ventricle (6.2 cm). His symptoms improved after permanent pacemaker implantation and he was scheduled to do follow-up every 6 months for serial echocardiographic testing with an assessment of left ventricular function and size.

His father (II-5) was admitted to hospital for repetitive lightheadedness and had several episodes of amaurosis in 2012. He was diagnosed with sick sinus syndrome for ambulatory ECG indicating an average heart rate of 48bpm, lowest heart rate of 24 bpm and longest RR interval of 2.7 s. Echocardiography revealed normal LVEF (60.0%) with enlargement of the left atrium (left atrial diameter 4.5 cm) and normal ventricle (LVDd 5.3 cm). A permanent pacemaker was implanted in 2012 and worked well during the follow-ups. His father recalled the sudden death of 4 family members (I-2, II-1, II-2, and II-4), which was described as "heart disease." And 2 of them (II-1, II-2) died before adulthood. The aunt (II-8) of the proband also had permanent pacemaker implantation for sick sinus syndrome in our hospital in 2010. Her ambulatory ECG before pacer maker implant showed atrial fibrillation with an average heart rate of 47bpm, lowest heart rate of 24 bpm and longest RR interval of 4.3 seconds. Echocardiography also revealed left atrium enlargement (4.7 cm), left ventricle enlargement (5.7 cm) with intact LVEF (55%). Two sisters (III -2 and III -3) have been diagnosed with CCD (1 for complete right bundle block and 1 for type-II second-degree AV block). There were 7 unaffected individuals in this family: the mother (II-6), 2 uncles (II-3 and II-7), 1 aunt (II-9), 1 sister (III -1), 1 brother (III -4), the wife (III -6), and son (IV-1) of the proband (Clinical characteristics of family individuals are shown in Table 1). They

Table 2

Genetic variants identified after whole-exome sequencing followed by adequate filtering.

Chr	Position	Gene	Transcript	Exon	Nucleotide change	Amino acid change	Associated diseases
1	156104642	*LMNA*	*NM_001282625*	4	c.686T>C	p.229I>T	DCM-1A, LGMD-1B
7	91712478	*AKAP9*	*NA*	NA	IVS32–6T>A	Splicing position	LQTS-11
2	179594481	*TTN*	*NM_133437*	63	c.18499G>C	p.6167G>R	DCM-1G
2	179581824	*TTN*	*NM_003319*	88	c.25637A>G	p.8546Q>R	DCM 1G
2	179401293	*TTN*	*NM_004415*	357	c.100181G>A	p.33394G>D	DCM 1G
1	3334515	*PRDM16*	*NM_022114*	11	c.2815C>G	p.939L>V	NVM, DCM 1LL
14	23890208	*MYH7*	*NM_000257*	25	c.3295G>T	p.1099A>S	DCM 1S

DCM = dilated cardiomyopathy, LGMD = limb girdle muscular dystrophy, LQTS = long QT syndrome, NVM = noncompaction of the ventricular myocardium.

were all healthy with normal ECGs and echocardiograms. Overall, the pattern of transmission is highly suggestive of autosomal dominant.

3.2. Identification of a novel mutation in LMNA by NGS

The NGS captured 99.5% of the target region with reaching mean coverage of 307×. We covered 92.7% of the targeted region in the mean read depth of at least 20× (range, 12–565X). The NGS revealed 289 genetic variants in the index patient in total. After filtering synonymous variants and MAF >0.2%, 0.4%, 0.05%, respectively for HCM, DCM, and ARVC in variant databases, a total of 7 missense variants were identified (Table 2). A novel missense mutation (c.686T>C, I229T) in exon 5 of the *LMNA* gene (chr1:156104642) leading to amino acid alteration (I229T, Fig. 2) was predicted to be "damaging" according to Provean, Sift, MutationTaster, M-CAP, and REVEL. The I229T variant in LMNA was in an extremely conserved region (Fig. 3). Then, we sequenced LMNA genes in the other affected CCD family members and confirmed the identical LMNA mutation (c.686T>C, I229T). Associations between genotype and phenotype were clinically identified, within all 5 affected CCD family members. This novel mutation has not been reported previously and was not found in the 1,000 genomes, dbSNP, ESP, ExAC, and Chigene in-house MAFs database, nor in the 535 healthy control individuals in the study.

Additionally, the NGS left us with other 6 genetic variants (Table 2). Mutation in A-kinase anchoring protein 9 (AKAP9) (chr7:91712478) was a missense mutation found in the non-coding region (IVS32–6T>A) and predicted as "probably influencing mRNA splicing" by functional annotation algorithms. Other identified mutations, including PRDM16 (chr1:3334515, p.939L>V), MYH7 (chr14:23890208, p.1099A>S), are predicted as "probably damaging." We also revealed 3 TTN mutations: TTN (chr2:179594481, p.6167G>R), TTN (chr2:179581824, p.8546Q>R), and TTN (chr2:179401293, p.33394G>D). They were all predicted as "damaging" according to all algorithms.

3.3. Sanger sequencing confirmation in family members

All the candidate pathogenic mutations were confirmed by Sanger sequencing. All the affected CCD individuals in the investigated family carried the same LMNA mutation. However, the association between the other 6 mutations and the CCD phenotype was undefined, for the pedigree is small and some family members were unavailable.

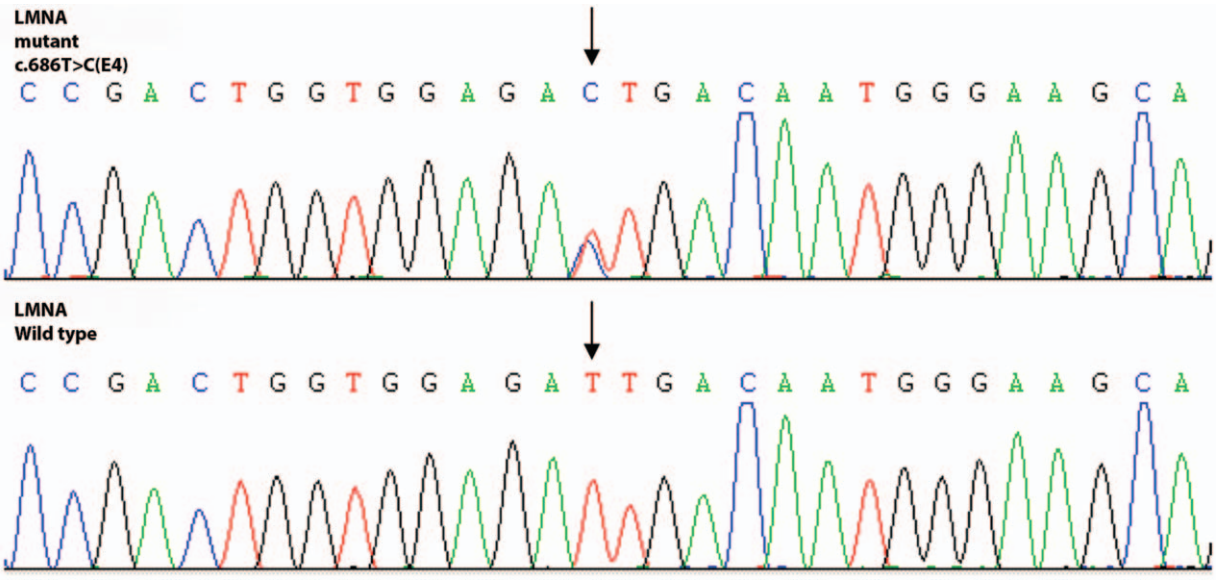

Figure 2. Electropherograms illustrating the heterozygous missense mutation (chr1:156104642, c.686 T>C, I229T) and a wild-type of control sequence. chr = chromosome, I = isoleucine, T = threonine.

LMNA_Mutant	RHETRLVE**T**DNGRQQEFESR
LMNA_Human	RHETRLVE**I**DNGRQQEFESR
LMNA_Chimpanzee	RHETRLVE**I**DNGKQREFESR
LMNA_Cow	RHETRLVE**I**DNGKQREFESR
LMNA_Dog	RHETRLVE**I**DNGKQREFESR
LMNA_Elephant	RHETRLVE**I**DNGKQREFESR
LMNA_Mouse	RHETRLVE**I**DNGKQREFESR
LMNA_Rat	RHETRLVE**I**DNGKQREFESR
LMNA_Pig	RHETRLVE**I**DNGKQREFESR
LMNA_Chicken	RHETRLVE**I**DNGRQQEFESK
LMNA_Rabbit	RHETRLVE**I**DNGKQREFESR

Figure 3. Alignment of homologous LMNA protein residue (p.229, Isoleucine). Amino acid conservation for the targeted region of LMNA. p = position.

3.4. Mutation results analysis

The Lamin A/C wildtype (green) and I229T mutant (rose red) were both showed in surface mode and the key residues Ile-229 and Thr-229 were colored in blue. Compared Figure 4A and B, we showed that the mutation of the 229-position from isoleucine to threonine could form a small cavity in the middle of the Lamin A/C I229T mutant (Fig. 2), which made the differences between the wild-type and the mutant.

3.5. Molecular docking results analysis

The interaction between the human PRC2 (green) and the Lamin A/C wildtype (rose red) was shown in Figure 5. Detailed analysis showed that an electrostatic interaction was observed between the residue Arg-201 of the PRC2 and the glutamic acid-rich domain consisted of the residues Glu-213, Glu-214, and Glu-217 of the Lamin A/C wildtype (Fig. 5A). In addition, the residues Asp-202 and Glu-394 of the PRC2 formed electrostatic interactions with the residues Arg-211 and Arg-196 of the Lamin A/C wildtype, respectively. Importantly, 2 hydrogen bond interactions were shown between the residue Asn-157 of the PRC2 and the residue His-222 of the Lamin A/C wildtype (bond length: 3.0 Å), the residue Phe-372 of the PRC2 and the residue Tyr-211 of the Lamin A/C wildtype (bond lengths: 3.0 Å), which were the main binding affinity between the PRC2 and the Lamin A/C wildtype.

To explain the activity difference of Lamin A/C wildtype and I229T mutant against PRC2, Lamin A/C I229T mutant was then docked into the binding site of PRC2, and the theoretical binding mode between Lamin A/C I229T mutant and PRC2 was shown in Figure 5B. We discovered an extra hydrogen bond between the

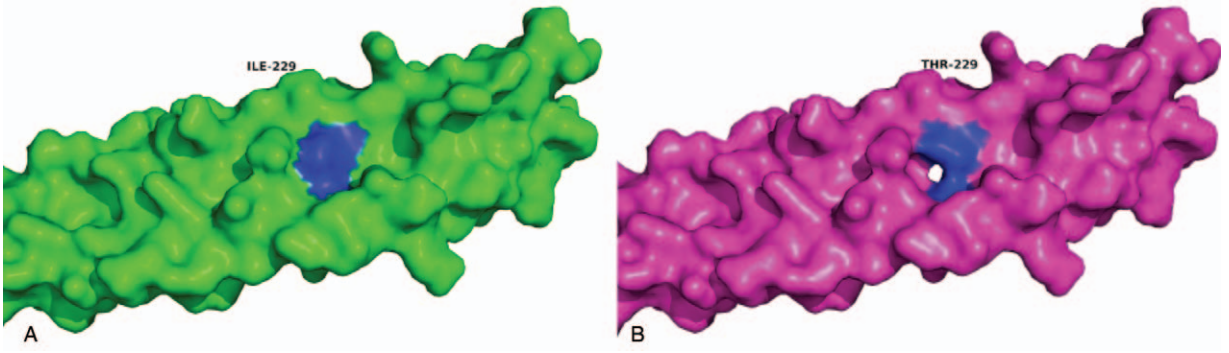

Figure 4. Lamin A/C protein structure. (A) The lamin A/C wildtype was showed in surface mode (green); the residue Ile-229 was colored in blue. (B) The lamin A/C I229T mutant was showed in surface mode (rose red); the residue Thr-229 was colored in blue. chr = chromosome, I = isoleucine, T = threonine.

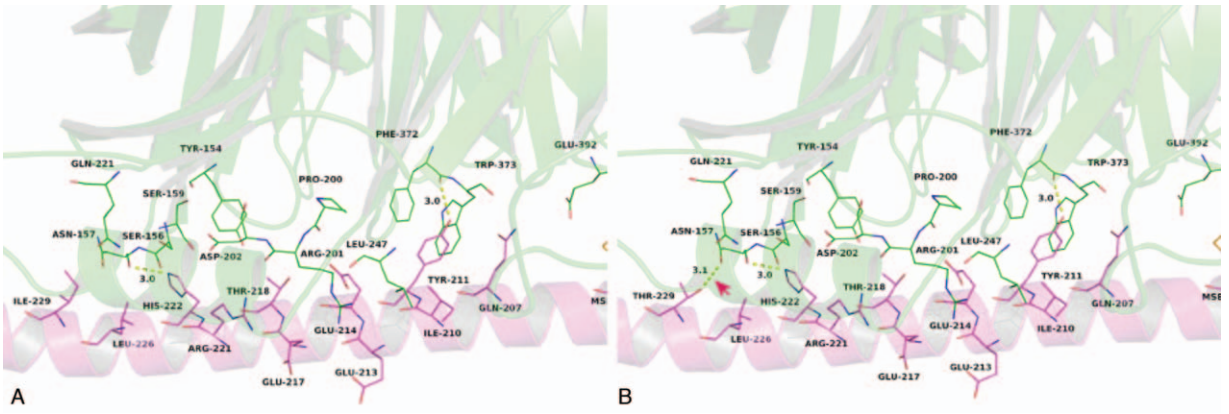

Figure 5. Molecular docking. (A) Detailed view of the interaction between the PRC2 (green) and lamin A/C wildtype (rose red). (B) Detailed view of the interaction between the PRC2 (green) and lamin A/C I229T mutant (rose red). An extra hydrogen bond between the residue Thr-229 of the lamin A/C mutant and the residue Asn-157 of PRC2 (*arrow*). Asn = asparagine, I = isoleucine, PRC2 = polycomb repressive complex 2, T, Thr = threonine.

residue Thr-229 of the Lamin A/C mutant and the residue Asn-157 of PRC2, which made Lamin A/C I229T mutant more active than Lamin A/C wildtype against PRC2. In addition, the estimated ZDOCK scores were 1210 for Lamin A/C wildtype and 1237 for Lamin A/C I229T mutant, respectively.

In conclusion, the above molecular simulations give us a rational explanation of the interaction between the PRC2 and the Lamin A/C (wildtype and I229T mutant), which provided valuable information for further study of binding sites between the PRC2 and the Lamin A/C.

4. Discussion

4.1. Genetic and clinical feature of LMNA-associated cardiomyopathy

LMNA-associated cardiomyopathy often occurs with CCDs, including sick sinus syndrome, heart block, supraventricular arrhythmias, and progressive ventricular arrhythmias.[1,13,14] In the Chinese family we investigated, 5 affected individuals with LMNA mutation all presented as CCDs, and one of them also has a tendency of heart enlargement. LMNA mutation is related to about 10% of cases of DCM with an age-related onset between the ages of 30 and 40.[15] It is also observed DCM onset can occur at any point in the development of CCD, but usually a few years after conduction system disease. LMNA-associated cardiomyopathy often leads to progressive heart failure, with an untreated sudden cardiac death rate of 46%.[5] Such DCM patients with the genetic predisposition may need implantable cardioverter-defibrillator therapy for primary prevention. Additionally, LMNA mutations are correlated with several other diseases, including skeletal myopathy, lipodystrophy, axonal neuropathy, and hypergonadotropic hypogonadism.

Most disease-causing LMNA mutations are missense mutations, although all mutations patterns have been reported (nonsense, frameshift, and intragenic deletions and duplications). Mutational landscape of LMNA illustrates all exons and the first 10 introns cause cardiac diseases[16] and the severity of LMNA cardiopathy is based on the amino acid changes. Arbustini et al demonstrated the clinical phenotype of LMNA (p.Arg331Gln) founder mutation has lower clinical risks and more benign than other reminiscent variants.[17] The missense mutation in LMNA (c.686T>C) identified in the investigated family here leads to an alteration of isoleucine to threonine (Fig. 2). Such variant is absent from databases and is predicted in silico to cause structural alteration in lamins with strong evidence for genetic pathogenesis. To date, mutations in LMNA are well known to cause autosomal dominant severe cardiac abnormalities, with the prevalence of 10% of DCM. However, the mechanisms of the pathogenesis of conduction system abnormalities and DCM are currently unclear, which need then to be investigated.

4.2. Possible mechanisms of disease

LMNA gene encodes intermediate filament proteins Lamins A/C which provide essential mechanical support in the nuclear envelope. Proteins Lamin B1/B2 are encoded by LMNB genes, whereas not reported to cause cardiac disease. Lamins are implicated in mitosis, chromatin organization, DNA replication, transcription, signal transduction, and cell-cycle regulation.[13,18,19] The pathogenicity of LMNA mutation can lead to lamins dysfunction, which potentially due to haploinsufficiency and/or LMNA overexpression. Overexpression of LMNA is identified to cause deleterious aggregation of lamins molecules at the peripheral region of the nuclear envelopes, which interfere with the nuclear functions. Ahn et al demonstrated stronger or weaker chemical interactions within adjacent amino acid residues were responsible for pathological lamins states, which led to deteriorating dynamic remodeling and incorrect mesh formation for the robust nuclear envelope.[20] The novel amino acid alteration we revealed locate in P.229 of exome 5, the flanking linker of the central rod domain close proximity to the α-helix bending region (p.331). In silico analysis, the mutation in LMNA (I229T) could form a small cavity in the middle of the Lamin A/C molecule. It is plausible to speculate I229T mutation may increase structural instability, thus influence protein inter-helical structure.

Several pathways have been revealed to be involved in LMNA-associated cardiac diseases. Recently, Salvarani et al employed pluripotent stem cell-derived cardiomyocytes (iPSC-CMs) carrying heterozygous K219T mutation on LMNA and demonstrated downregulated Nav1.5 channel expression, decreased sodium current density and slower conduction velocity. They revealed mutant Lamin A/C had a higher binding affinity for PRC2, which can lead to the methylation of lysine 27 on histone 3 and thus silence Nav1.5 channel expression.[21] For the close proximity between I229T and K219T, we construct molecular docking to analyze the interaction between human PRC2 and I229T-lamin A/C. In silico, the interaction between Lamin A/C I229T mutant and PRC2 was similar to the Lamin A/C wildtype. The only difference was that the residue Thr-229 of the Lamin A/C mutant formed an extra hydrogen bond with the residue Asn-157 of PRC2. The estimated ZDOCK scores were 1210 for Lamin A/C wildtype and 1237 for Lamin A/C I229T mutant, respectively. These findings support the hypothesis that mutant I229T-lamin A/C and PRC2 also bind together with higher affinity than Lamin A/C wildtype, thus providing useful information or future validation in the cellular model.

In addition, Lee et al modeled induced iPSC-CMs from a large LMNA-associated DCM family cohort (348–349insG, K117fs) and discovered overactivation of platelet-derived growth factor (PDGF) signaling pathway.[22] They demonstrated PDGF signaling pathway inhibition alleviates the arrhythmogenicity of mutant iPSC-CMs in vitro, thus suggested PDGF receptor-β as a potential therapeutic target. Their findings replenished the pathophysiological mechanism of conduction abnormalities related to LMNA-associated cardiomyopathy.

Choi et al found that the AKT-mechanistic target of rapamycin signaling was hyperactivated in the hearts of LMNA (H222P knock-in) mice, thus demonstrated the defective autophagy of LMNA-associated DCM.[23] Muchir et al revealed the abnormal activation of the extracellular signal-regulated kinase (ERK) in mitogen-activated protein kinase (MAPK) signaling pathway in vivo through LMNA (H222P knock-in) mutation mice. They treated mutant mice that develop cardiomyopathy with an inhibitor of ERK activation (PD98059) and showed a significant delay of left ventricle dilation.[24] Several oral drugs that target mechanistic target of rapamycin and MAPK pathways have been put in clinical development. Selumetinib, an allosteric inhibitor of MEK1/2 inhibitors (inhibit MAPK kinase) shows the most promising future. Results from previous studies have revealed ERK is activated through phosphorylation by the receptor tyrosine

kinases.[25,26] Lamins form various fibrous structures in the nuclear lamina and may serve as a scaffold for substrates of ERK phosphorylation during upstream receptor activation. It is possible that the change of lamins structure resulting from LMNA mutations may alter the interaction between lamins and ERK, thus influence ERK phosphorylation. The concrete mechanism of how lamins interact with the ERK pathway is intriguing, future studies are still needed.

4.3. Possible modifying effects of other genetic variants

Among the other 6 genetic variants in our study, mutations of AKAP9 (IVS32-6T>A), PRDM16 (p.939L>V), and MYH7 (p.1099A>S) have the uncertainty of pathogenicity according to functional prediction. A-kinase anchoring proteins are a group of scaffolding protein that is fundamental to ensure the accuracy of signal transduction of protein kinase A pathway.[27] AKAP9 mutations were previously identified to be related to congenital cardiac arrhythmias.[28–30] Cardiac repolarization may be impeded by defective slow-activating delayed potassium current resulting from AKAP9 mutations that cause congenital Long-QT syndrome. Furthermore, De Villiers et al found intronic AKAP9 polymorphisms also have modifying effects on cardiac diseases.[28] We identified the same AKAP9 mutation (IVS32-6T>A) in the proband and his mother (II-6), and such the intronic mutation may influencing mRNA splicing.

Additionally, 3 TTN mutations (p.6167G>R, p.8546Q>R, p.33394G>D) in the investigated family, were predicted to modify cardiac disease. TTN is the largest human gene and accounts for >20% of the total target region.[31] Nonsense, frameshift, splicing, and copy-number mutations of TTN are demonstrated to cause protein truncation, whereas pathogenic missense mutations are rarely reported.[32] Whether such genetic variants have possible modifying effects to LMNA mutation carriers is unknown for the relatively small family pedigree and other family members were unavailable. Supplementary Table 1, http://links.lww.com/MD/E725.

5. Limitations

First, instead of a hypothesis-free approach, the targeted NGS covered all known pathogenic genes related to cardiomyopathy and channelopathy. Furthermore, the targeted NGS is unable to interrogate the genomic structural variations comprehensively. Though we design several algorithms to predict structural variations, it still insufficient to identify variations by sequencing data.

Second, we cannot obtain heart tissue samples of LMNA mutation carriers to perform functional analyses because either myocardial biopsy or heart transplantation was not indicated and none of these patients received postmortem examination.

Third, because of the relatively small family and presence of several unavailable family members, we cannot fully elucidate the modifying effect of other possible genetic variants.

6. Conclusion

We report a novel heterozygous I229T mutation on LMNA associated with familial CCD from a consanguineous Chinese family. Through molecular docking, additional electrostatic interactions were found between human PRC2 and I229T-lamin A/C, which possible increase methylation of lysine 27 on histone 3 and thus silence Nav1.5 channel expression. Future molecular researches are needed to validate this hypothesis.

Author contributions

Conceptualization: Wei Xu.
Data curation: Wei Xu.
Formal analysis: Wei Xu.
Methodology: Wei Xu.

References

[1] Arbustini E, Pilotto A, Repetto A, et al. Autosomal dominant dilated cardiomyopathy with atrioventricular block: a lamin A/C defect-related disease. J Am Coll Cardiol 2002;39:981–90.
[2] Fatkin D, MacRae C, Sasaki T, et al. Missense mutations in the rod domain of the lamin A/C gene as causes of dilated cardiomyopathy and conduction-system disease. N Engl J Med 1999;341:1715–24.
[3] Hershberger RE, Hanson EL, Jakobs PM, et al. A novel lamin A/C mutation in a family with dilated cardiomyopathy, prominent conduction system disease, and need for permanent pacemaker implantation. Am Heart J 2002;144:1081–6.
[4] Brodt C, Siegfried JD, Hofmeyer M, et al. Temporal relationship of conduction system disease and ventricular dysfunction in LMNA cardiomyopathy. J Card Fail 2013;19:233–9.
[5] van Berlo JH, de Voogt WG, van der Kooi AJ, et al. Meta-analysis of clinical characteristics of 299 carriers of LMNA gene mutations: do lamin A/C mutations portend a high risk of sudden death? J Mol Med (Berl) 2005;83:79–83.
[6] Argiriou M, Kolokotron SM, Sakellaridis T, et al. Right heart failure post left ventricular assist device implantation. J Thorac Dis 2014;6(Suppl 1):S52–9.
[7] van Rijsingen IA, Bakker A, Azim D, et al. Lamin A/C mutation is independently associated with an increased risk of arterial and venous thromboembolic complications. Int J Cardiol 2013;168:472–7.
[8] Kusumoto FM, Schoenfeld MH, Barrett C, et al. 2018 ACC/AHA/HRS guideline on the evaluation and management of patients with bradycardia and cardiac conduction delay: a report of the American College of Cardiology/American Heart Association Task Force on Clinical Practice Guidelines and the Heart Rhythm Society. J Am Coll Cardiol 2019;74:e51–156.
[9] Yancy CW, Jessup M, Bozkurt B, et al. 2013 ACCF/AHA guideline for the management of heart failure: a report of the American College of Cardiology Foundation/American Heart Association Task Force on Practice Guidelines. J Am Coll Cardiol 2013;62:e147–239.
[10] Richardson P, McKenna W, Bristow M, et al. Report of the 1995 World Health Organization/International Society and Federation of Cardiology Task Force on the Definition and Classification of cardiomyopathies. Circulation 1996;93:841–2.
[11] Li H, Durbin R. Fast and accurate long-read alignment with Burrows-Wheeler transform. Bioinformatics 2010;26:589–95.
[12] De Summa S, Malerba G, Pinto R, et al. GATK hard filtering: tunable parameters to improve variant calling for next generation sequencing targeted gene panel data. BMC Bioinformatics 2017;18(Suppl 5):119.
[13] Brodsky GL, Muntoni F, Miocic S, et al. Lamin A/C gene mutation associated with dilated cardiomyopathy with variable skeletal muscle involvement. Circulation 2000;101:473–6.
[14] Parks SB, Kushner JD, Nauman D, et al. Lamin A/C mutation analysis in a cohort of 324 unrelated patients with idiopathic or familial dilated cardiomyopathy. Am Heart J 2008;156:161–9.
[15] Hershberger RE, Hedges DJ, Morales A. Dilated cardiomyopathy: the complexity of a diverse genetic architecture. Nat Rev Cardiol 2013;10:531–47.
[16] Captur G, Arbustini E, Bonne G, et al. Lamin and the heart. Heart 2018;104:468–79.
[17] Arbustini E, Favalli V, Narula N. LMNA mutations associated with mild and late-onset phenotype: the case of the Dutch founder mutation p.(Arg331Gln). Circ Cardiovasc Genet 2017;10:
[18] Lee SJ, Jung YS, Yoon MH, et al. Interruption of progerin-lamin A/C binding ameliorates Hutchinson-Gilford progeria syndrome phenotype. J Clin Invest 2016;126:3879–93.
[19] Burke B, Stewart CL. The nuclear lamins: flexibility in function. Nat Rev Mol Cell Biol 2013;14:13–24.
[20] Ahn J, Jo I, Kang SM, et al. Structural basis for lamin assembly at the molecular level. Nat Commun 2019;10:3757.

[21] Salvarani N, Crasto S, Miragoli M, et al. The K219T-Lamin mutation induces conduction defects through epigenetic inhibition of SCN5A in human cardiac laminopathy. Nat Commun 2019;10:2267.
[22] Lee J, Termglinchan V, Diecke S, et al. Activation of PDGF pathway links LMNA mutation to dilated cardiomyopathy. Nature 2019;572:335–40.
[23] Choi JC, Worman HJ. Reactivation of autophagy ameliorates LMNA cardiomyopathy. Autophagy 2013;9:110–1.
[24] Muchir A, Wu W, Choi JC, et al. Abnormal p38alpha mitogen-activated protein kinase signaling in dilated cardiomyopathy caused by lamin A/C gene mutation. Hum Mol Genet 2012;21:4325–33.
[25] Muchir A, Pavlidis P, Decostre V, et al. Activation of MAPK pathways links LMNA mutations to cardiomyopathy in Emery-Dreifuss muscular dystrophy. J Clin Invest 2007;117:1282–93.
[26] Malarkey K, Belham CM, Paul A, et al. The regulation of tyrosine kinase signalling pathways by growth factor and G-protein-coupled receptors. Biochem J 1995;309:361–75.
[27] Suryavanshi SV, Jadhav SM, McConnell BK. Polymorphisms/mutations in A-kinase anchoring proteins (AKAPs): role in the cardiovascular system. J Cardiovasc Dev Dis 2018;5:
[28] de Villiers CP, van der Merwe L, Crotti L, et al. AKAP9 is a genetic modifier of congenital long-QT syndrome type 1. Circ Cardiovasc Genet 2014;7:599–606.
[29] Chen L, Marquardt ML, Tester DJ, et al. Mutation of an A-kinase-anchoring protein causes long-QT syndrome. Proc Natl Acad Sci U S A 2007;104:20990–5.
[30] Ramirez AH, Shaffer CM, Delaney JT, et al. Novel rare variants in congenital cardiac arrhythmia genes are frequent in drug-induced torsades de pointes. Pharmacogenomics J 2013;13:325–9.
[31] Haas J, Frese KS, Peil B, et al. Atlas of the clinical genetics of human dilated cardiomyopathy. Eur Heart J 2015;36:1123–35a.
[32] Herman DS, Lam L, Taylor MR, et al. Truncations of titin causing dilated cardiomyopathy. N Engl J Med 2012;366:619–28.